Experimental and theoretical study of the gas phase reaction of ethynyl radical with methane (HCC+CH4)

ARTICLE *in* CHEMICAL PHYSICS LETTERS · OCTOBER 2000

Impact Factor: 1.9 · DOI: 10.1016/S0009-2614(00)01033-2

27 October 2000

ELSEVIER

Chemical Physics Letters 329 (2000) 412–420

CHEMICAL PHYSICS LETTERS

www.elsevier.nl/locate/cplett

Experimental and theoretical study of the gas phase reaction of ethynyl radical with methane ($HC{\equiv}C + CH_4$)

Benny Ceursters, Hue Minh Thi Nguyen [1], Jozef Peeters, Minh Tho Nguyen *

Department of Chemistry, University of Leuven, Celestijnenlaan 200F, B-3001 Leuven, Belgium

Received 3 July 2000; in final form 8 September 2000

Abstract

Absolute rate coefficients of the reaction of ethynyl radical with methane were measured for the first time at higher temperatures by a pulsed laser photolysis/chemiluminescence (PLP/CL) technique. Ethynyl radicals (HCC) radicals were generated pulsewise upon excimer laser photodissociation of acetylene at 193 nm and pseudo-first-order exponential decays of thermalized HCC were monitored in real-time by the $CH(A^2\Delta \rightarrow X^2\Pi)$ chemiluminescence produced by their reaction with O_2. The rate coefficients $k(HCC + CH_4)$, over $295 \leqslant T\ (K) < 800$, exhibit strong non-Arrhenius behaviour, being $k(T) = 1.39 \times 10^{-18} T^{2.34\pm0.40} \exp[(380 \pm 180)\ K/T]$ cm^3 molecule^{-1} s^{-1}. Calculations at the CCSD(T)/aug-cc-pvTZ level reveal that the direct H-abstraction yielding $HC{\equiv}CH + CH_3$ has the lowest energy barrier of about 10 kJ mol^{-1}.

1. Introduction

Ethynyl radicals (HCC) are primary products of the decomposition of acetylene. As a result, there has been considerable interest in their reactions occurring in several different environments, both natural and man-made, containing acetylene. The abundance of HCC in interstellar space [1,2] and planetary atmospheres (such as Titan's) [3,4] has motivated recent studies of their low-temperature kinetics [5,6]. Also, HCC plays a crucial role in hydrocarbon combustion processes in which it is involved in the formation of diacetylene (C_4H_2) and the higher polyacetylenes ($C_{2n}H_n$), as well as of polycyclic aromatic hydrocarbons (PAHs) and hence of soot [7–15]. In fact, in fuel-rich near-sooting flames, the fraction of primary fuel that passes through C_4H_2 can amount up to 50% [9,10]. Furthermore, ethynyl radicals react fast with NO yielding $HCN + CO$ or $CN + HCO$ as likely products [16–18] and as such, they may intervene in NO_x subchemistry in conditions, where HCC is an important intermediate, i.e., in fuel-rich hydrocarbon flames in general and in high-temperature 'NO-reburning' in particular [19].

Therefore, detailed and quantitative kinetic/mechanistic information about potentially important formation and destruction reactions of HCC over a broad temperature range is of fundamental chemical importance. In this work, we set out to investigate the reactivity of ethynyl radicals towards methane using both experimental and theoretical approaches. Although the kinetics have

* Corresponding author.

E-mail addresses: jozef.peeters@chem.kuleuven.ac.be (J. Peeters), minh.nguyen@chem.kuleuven.ac.be (M.T. Nguyen).

[1] On leave from Faculty of Chemistry, National University of Education, Hanoi, Vietnam.

0009-2614/00/$ - see front matter
PII: S0009-2614(00)01033-2

been studied by a number of authors [5,6,16,20–25], most of these studies were at a single temperature, near ambient, and rate coefficients were often determined in an indirect or relative way. In the only measurement covering a wider range of low-temperatures ($T = 154$–359 K), using transient infrared laser absorption spectroscopy, Opansky and Leone [5,6] derived the following absolute rate constant at $T = 298 \pm 2$ K : $k(\mathrm{HCC} + \mathrm{CH_4}) = (2.3 \pm 0.1) \times 10^{-12}$ cm^3 molecule^{-1} s^{-1}. This value is consistent with earlier results obtained by various groups ranging from 1.2×10^{-12} to 4.5×10^{-12} cm^{-3} molecule^{-1} s^{-1} at the same temperature [5,6,16,20–25]. The primary aim of the present work was to determine the absolute rate coefficient over the $T = 295$–800 K region. Use was made of a pulsed laser photolysis/chemiluminescence (PLP/CL) technique, our version of which was validated earlier [17,26,27] as a very precise, accurate, flexible and therefore highly useful tool for studying the gas-phase kinetics of the HCC($X^2\Sigma^+$) radical, both for reactions with an appreciable energy barrier [17] and barrier-free processes [27]. In addition, the experimental study was supplemented by ab initio calculations of the transition structures for possible reactions that thus allow the most favoured transformation to be identified.

2. Experimental results

The instrumental setup in the PLP/CL experiments is similar to that used in our earlier HCC kinetic studies [17,26,27]; it is part of a PLP/LIF setup described in detail previously [28,29].

In brief, ethynyl radicals were created pulsewise by continuously flowing a gas mixture of acetylene, molecular oxygen, methane and helium through a cylindrical quartz tube towards a photolysis cell and photolyzing the C_2H_2 using the 193 nm output of an ArF excimer laser (30 mJ/pulse at 10 Hz) with the beam section sized down to 8 mm × 3 mm. The real-time pseudo-first-order decay of the HCC radicals was monitored by measuring the intensity $I(\mathrm{CH}^*)$ of the 430 nm $\mathrm{CH}(A^2\Delta \rightarrow X^2\Pi)$ chemiluminescence [26,30–32] resulting from their reaction with O_2, present in a large and constant concentration (Eq. (1)) [27]:

$$\begin{aligned} \mathrm{HCC} + \mathrm{O_2} &\rightarrow \text{products} \\ &\rightarrow \mathrm{CH}(A^2\Delta) + \mathrm{CO_2} \\ &\quad\downarrow \\ &\mathrm{CH}(X^2\Pi) + h\nu(\lambda = 430\ \mathrm{nm}) \end{aligned} \qquad (1)$$

Given the quasi-steady state for $\mathrm{CH}(A^2\Delta)$ in the experimental conditions, the chemiluminescence signal, $I(\mathrm{CH}^*)$, is directly proportional to the ethynyl concentration. The chemiluminescence was collected perpendicular to the laser beam axis by means of suitable collection optics. Before entering a photomultiplier tube (PMT), the chemiluminescence passed through a narrow-bandpass interference filter ($\lambda = 430 \pm 10$ nm) to select the spectral region of interest. The output of the PMT was fed to a boxcar integrator. The delay between the laser firing and the opening of the 1 μs wide boxcar gate was gradually increased after each laser pulse at a rate of 0.1 μs s^{-1}. The reaction cell employed in this work was equipped with an inner ceramic tube (Al_2O_3 99.7% with internal gray SiC coating) with a Ni/Cr resistive wire coil, enabling the gas mixture flowing (slowly) through the tube to be heated to 800 K. The temperature in the small observed reaction volume (8 mm × 3 mm × 10 mm) at the center of the cell was monitored by a movable calibrated chromel/alumel thermocouple. All gases were obtained commercially, and the purities where as follows: He 99.9990%, O_2 99.995%, CH_4 99.95% (all AIR LIQUIDE) and C_2H_2 99.5% (HOEK LOOS). Since commercial acetylene contains acetone, it was purified before use by passing it through a dry ice/acetone trap. The flow rates of the gases were regulated and measured by calibrated mass flow controllers. The total gas flow rate was sufficient to refresh the gas in the observed volume between two successive laser shots. The concentrations of the species were determined from their partial flows and from the total reactor pressure. Kinetic experiments were performed at an acetylene number density of $(4.556.37) \times 10^{14}$ molecules cm^{-3}, an O_2 concentration of $(4.04 - 6.40) \times 10^{15}$molecules cm^{-3} and varying CH_4 number densities in the range $(0$–$3.33) \times 10^{16}$ molecules cm^{-3}. In the experiments, the reactants C_2H_2, O_2

and CH_4 were always present in a very large excess over HCC (initial ethynyl concentration of about 10^{12} molecules cm^{-3}) such that any contribution from secondary and/or radical–radical reactions to the HCC decay could be neglected. In addition, HCC removal out of the irradiated/observed volume by diffusion and/or convection occurs on a time scale of milliseconds in the experimental conditions and cannot possibly compete with its loss by chemical reaction on a time scale of microseconds.

Because pseudo-first-order decay obtains, due to reactions of HCC with CH_4, C_2H_2 and O_2, the decay of HCC can be expressed by:

$$[\mathrm{HCC}]_t = [\mathrm{HCC}]_0 \exp(-k't) \quad (2)$$

with

$$k' = k_{\mathrm{methane}}[\mathrm{CH_4}] + k_{\mathrm{acetylene}}[\mathrm{C_2H_2}] + k_{\mathrm{oxygen}}[\mathrm{O_2}] \quad (3)$$

The total bath gas pressure of 10 Torr He and the oxygen number densities $[O_2] \geqslant 4 \times 10^{15}$ molecules cm^{-3} ensure the complete thermalization of the HCC within the 5 μs period prior to the decay measurements, as was shown earlier [27]. As a further test, room temperature measurements were also performed at a higher total pressure, yielding identical results (see Table 1). An example of an HCC exponential decay is shown in Fig. 1. Bimolecular rate coefficients k_{methane} were determined by measuring the decay constant k' at varying $[CH_4]$ and at fixed $[C_2H_2]$ and $[O_2]$. The slope of the linear plot of k' vs $[CH_4]$ gives the rate coefficient of the reaction with methane, whereas the ordinate intercept is equal to the contributions of both precursor and oxygen to the total decay constant k': $k_{\mathrm{acetylene}}[C_2H_2] + k_{\mathrm{oxygen}}[O_2]$. A typical example of such a plot is shown in Fig. 2. The $k_{\mathrm{methane}}(517\ \mathrm{K})$ value obtained from the slope of this plot is $(6.2 \pm 0.6) \times 10^{-12}$ cm^3 $molecule^{-1}$ s^{-1}. The ordinate intercept (at $[CH_4] = 0$) of $(1.98 \pm 0.01) \times 10^5$ s^{-1} matches perfectly with the expected

Table 1
Bimolecular rate coefficients k_{methane} in cm^3 $molecule^{-1}$ s^{-1} for the reaction of HCC with CH_4

T (K)	$1000/T$ (K^{-1})	$k_{\mathrm{methane}} \times 10^{-12}$
295	3.39	2.91 ± 0.29
331	3.02	3.56 ± 0.36
351	2.85	3.71 ± 0.37
385	2.60	3.92 ± 0.39
415	2.41	4.29 ± 0.43
445	2.25	5.48 ± 0.55
517	1.93	6.23 ± 0.62
589	1.70	8.05± 0.81
704	1.42	10.5 ± 1.1
779	1.28	13.2 ± 1.3

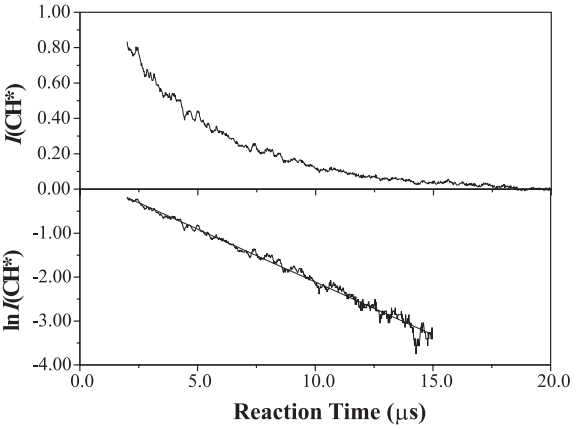

Fig. 1. Typical decay and semilog plot of the relative HCC concentration vs reaction time; $T = 517$ K; $p_{\mathrm{tot}} = 10$ Torr (He bath gas); $[C_2H_2] = 4.79 \times 10^{14}$ molecules cm^{-3}; $[O_2] = 4.81 \times 10^{15}$ molecules cm^{-3}; $[CH_4] = 6.04 \times 10^{15}$ molecules cm^{-3}. The straight line represents the weighted linear least-squares fit.

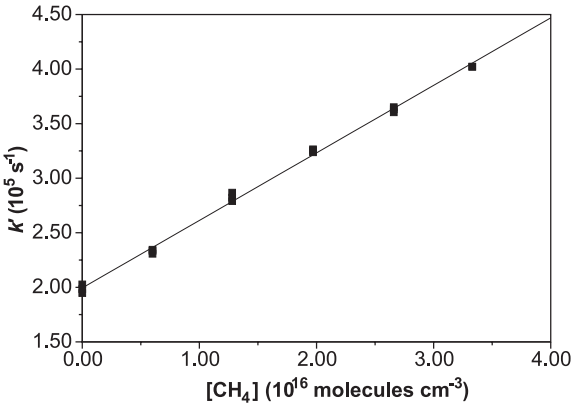

Fig. 2. Pseudo-first-order decay constants k' plotted vs $[CH_4]$ at $T = 517$ K; $p_{\mathrm{tot}} = 10$ Torr (He bath gas); $[C_2H_2] = 4.79 \times 10^{14}$ molecules cm^{-3}; $[O_2] = 4.81 \times 10^{15}$ molecules cm^{-3}. The solid line represents a weighted linear least-squares fit to the data points. The slope of the line yields $k_{\mathrm{methane}}(517\ \mathrm{K}) = (6.23 \pm 0.62) \times 10^{-12}$ cm^3 $molecule^{-1}$ s^{-1}.

value of $k_{\text{acetylene}}[C_2H_2] + k_{\text{oxygen}}[O_2] = (1.9 \pm 0.2) \times 10^5\ s^{-1}$, using our results $k_{\text{acetylene}}(517\ K) = 1.3 \times 10^{-10}$ and $k_{\text{oxygen}}(517\ K) = 2.6 \times 10^{-11}$ cm^3 molecule^{-1} s^{-1} [31,32]. Such internal consistency was observed at all temperatures.

Our complete set of k_{methane} data in the range $T = 295$–779 K is given in Table 1. The statistical error was 2–5%. The stated total errors, amounting to about 10%, include estimated maximum systematic errors due to inaccuracies in the absolute reactant concentrations and in other experimental parameters. Fig. 3 displays $\log k_{\text{methane}}$ vs $1000/T$. The plot features a strong non-Arrhenius behavior showing an upward curvature. A non-linear least-square analysis leads to the following three-parameter modified Arrhenius expression for the range 300–800 K.

$$k_{\text{methane}}(T) = 1.39 \times 10^{-18} T^{2.34 \pm 0.40} \times \exp[(380 \pm 180)\ \text{K}/T]\ \text{cm}^3\ \text{molecule}^{-1}\ \text{s}^{-1}.$$

Our value $k(T = 295\ \text{K}) = (2.9 \pm 0.2) \times 10^{-12}$ cm^3 molecule^{-1} s^{-1} is nearly identical to the average of 2.8×10^{-12} cm^3 molecule^{-1} s^{-1} of the six previous determinations, which range from 1.2×10^{-12} to 4.5×10^{-12} cm^3 molecule^{-1} s^{-1} [5,6,16,20–25].

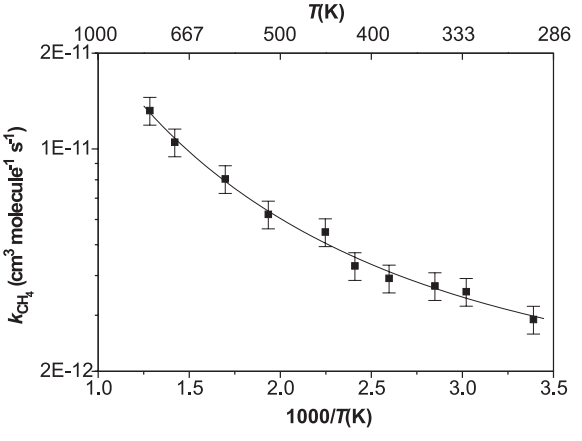

Fig. 3. Arrhenius plot showing the rate coefficients k methane obtained for the gas-phase reaction $HCC + CH_4$. The full curve represents a fit using a three-parameter modified Arrhenius expression. Error bars include possible systematic errors.

3. Quantum chemical calculations

Having established the rate coefficients of the $HCC + CH_4$ reaction for the first time over an extended range of higher temperatures, we now attempt to identify the most likely product channel using ab initio molecular orbital calculations. The (C_3H_5) system contains several low-energy isomers including methylvinyl and allyl radicals. It is not our intention here to explore fully this interesting potential energy surface. Our search was rather limited to the part of the energy surface comprising the reaction pathways starting from $HCC + CH_4$. That means that we were not searching for the connections between the products of the various possible pathways.

All calculations were performed using the GAUSSIAN94 suit of programs [33]. Geometry optimizations were initially conducted using molecular orbital theory at the Hartree–Fock (HF), second-order perturbation theory (MP2) and subsequently refined using coupled–cluster theory with all single and double excitations plus perturbative corrections for triple substitution (CC SD(T)) levels in conjunction with the 6-31G(d,p) atomic basis set. The unrestricted formalism (UHF, UMP2 and UCCSD) was used for open-shell states. Harmonic vibrational wave numbers were calculated at both UHF and UMP2 levels to characterize the stationary points as equilibrium and transition structures. The zero-point energies (ZPE) were derived from UMP2 frequencies scaled down by a uniform factor of 0.95. Electronic energies were further improved by single-point CCSD(T) calculations with the 6-311++G(d,p) basis set and MP2 calculations with the even larger 6-311++G(3df,2p) and aug-cc-pVTZ basis sets. In (U)MP2 and (U)CCSD(T) calculations, the core orbitals were kept frozen. The improved relative energies were then obtained using a simple additivity approximation (4) in which L stands for a large basis set, either 6-311++G(3df,2p) or aug-cc-pvTZ, and S for the smaller 6-311+G(d,p) set. We thus assume that the correlation energy accounted for in going from MP2 to CCSD(T) is the same for both small and large basis sets. The results obtained by both large basis sets are quite close to each other. To simplify the presentation of data,

only the CCSD(T)/aug-cc-pVTZ are given and referred to hereafter.

$$E(CCSD(T)/L) = E(MP2/L) + E(CCSD(T)/S) - E(MP2/S) \quad (4)$$

The ethynyl radical exhibits a $^2\Sigma^+$ electronic ground state in which the unpaired electron is mainly located in the 2pσ orbital of the terminal carbon atom. Upon bending, a certain amount of the unpaired electron is actually transferred to the central carbon in such a way that the latter could also act as a radical center. Due to the fact that the bending of HCC is a quite facile motion with a vibrational frequency of only 371 cm^{-1} [34], it seems reasonable to consider both carbon atoms of HCC as reactive radical sites. A priori, each radical center could either abstract or substitute a hydrogen of methane, or insert into one of its C–H bonds. In fact, we have been able to locate five (5) distinguishable transition structures (TS) connecting the starting point $HCC + CH_4$ **1** to different products. The selected geometrical paramaters of these TS's at both UMP2 and CCSD(T) level using the 6-31G(d,p) basis set are shown in Fig. 4. The latter include the two TS's for hydrogen abstraction **Ab/2** and **Ab/3**, the two TS's for hydrogen substitution **Sub/4** and **Sub/5** and finally the TS for C–H insertion **Ins/6**. As for a convention, the number **/x** ranging from **x = 2** to **6** indicates the corresponding products. To simplify the presentation of data, optimized geometries of the reactants and products are omitted here. They are rather simple and can readily be reproduced. Fig. 5 displays schematic energy profiles illustrating the reaction pathways.

Let us first examine the geometrical aspects of the TS's. The TS **Ab/2** is no doubt the most expected one, as HCC uses its terminal carbon to perform the H-abstraction producing CH_3+ HCCH **2**. A previous study using both UHF and UMP2 methods with various basis sets [35] reported a C_{3v} TS for this abstraction implying a linear C–H–C framework. On the contrary, our UMP2/6-31G(d,p) calculations indicate a significant deviation from the linearity (up to 13°) in TS **Ab/2**. Although this bending induces only a tiny

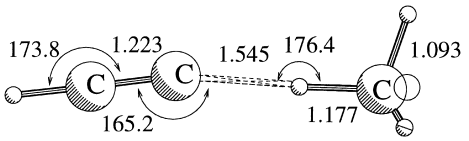

TS Ab/2

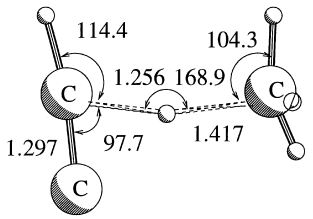

TS Ab/3

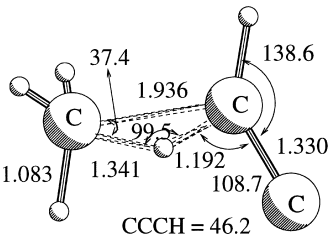

TS Ins/6

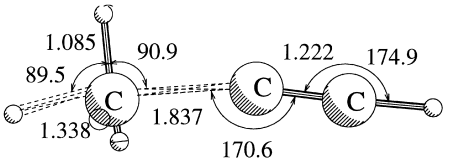

TS Sub/4

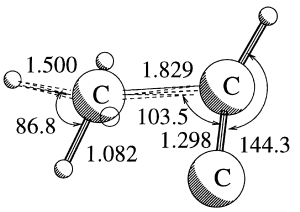

TS Sub/5

Fig. 4. Selected optimized geometrical parameters of five transition structures connecting to the $HCC + CH_4$ starting reactants **1** (UCCSD(T)/6-31G(d,p) values). Bond lengths are given in angstrom and bond angles in degree. See text for definition.

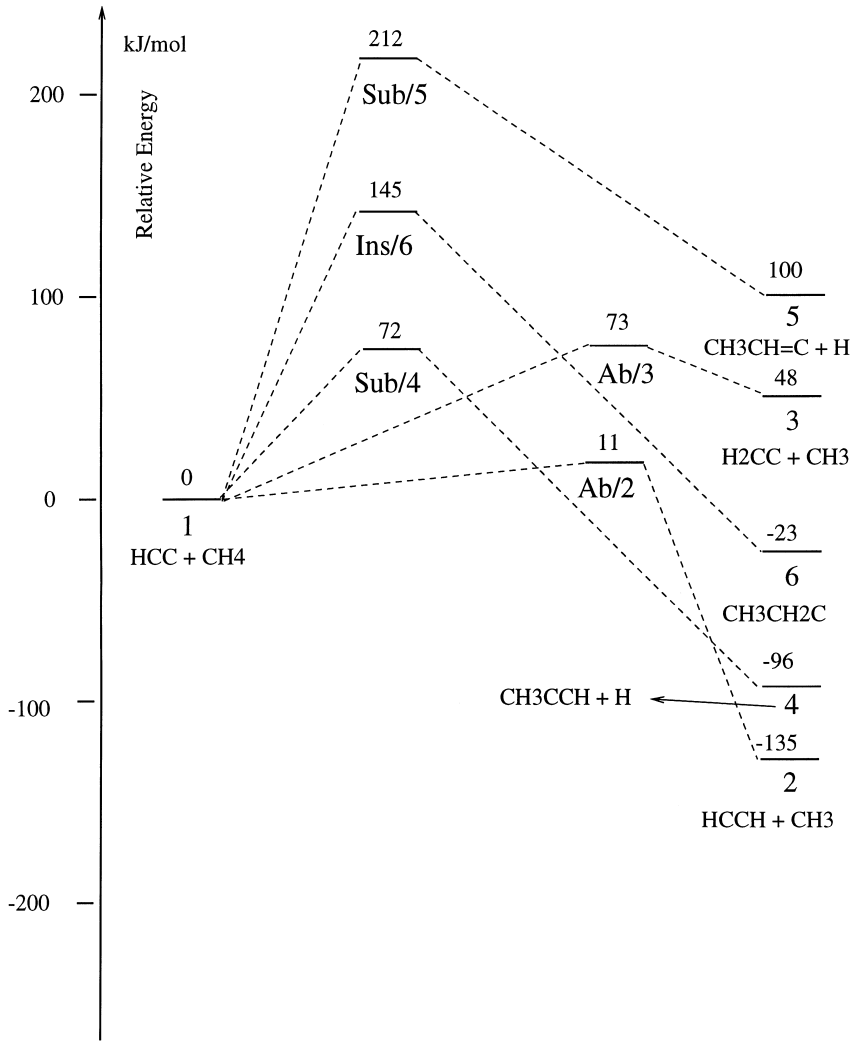

Fig. 5. Schematic potential energy profiles illustrating the different pathways of the HCC + CH_4 reaction. Relative energies given in kJ mol^{-1} are obtained from approximate CCSD(T)/aug-cc-pVTZ //CCSD(T)/6-31G(d,p) + ZPE.

energetic consequence, it could become appreciable in the kinetic treatments where the hindered internal rotational modes would have to be considered instead of degenerate vibrations. The CCSD(T) method suggests a more compact form of **Ab/2**. Nevertheless, we wish to stress that the basis set employed here is only of moderate quality; a strictly linear C–H–C framework in TS **Ab/2** could not be ruled out if larger basis set could be used. In accord with the large exothermicity of the abstraction, the methane C–H bond in **Ab/2** is only marginally stretched (1.13 Å vs 1.089 Å in methane). Similarly, the intermolecular C–H distance of 1.55 Å is also much larger than the corresponding of about 1.37 Å obtained at the UMP2 level for the H-abstraction from methane by the vinyl radical.

The second TS for H-abstraction **Ab/3** corresponds in fact to a radical attack of the central carbon generating CH_3 + $H_2C{=}C$ **3**. The C–H–C framework becomes now more bent (around 155–160°). Because vinylidene is a higher-energy isomer

of acetylene, according to the Hammond postulate, this TS is expected to lie higher in energy than **Ab/2**. In **Ab/3**, both C–H distances become more comparable in such a way that the migrating H atom lies in the middle of the C–C distance. This is indicative of the fact that both radical centers, HCC central carbon and methyl carbon, have somehow a similar radical reactivity, and in addition, the former could also be compared with vinyl carbon.

Perhaps both TS's **Sub/4** and **Sub/5** are less expected as they represent the substitution of a methane hydrogen by the ethynyl radical. In some respects, they resemble the TS of a nucleophilic substitution (SN_2) in which the entering and the departing groups are connected by an almost planar methyl moiety. It seems that the lack of a negative charge tends to destabilize this type of TS. It is worth mentioning that this type of process is not unprecedented. In a previous study on the $CH_3CO + Cl$ reaction [36], we found indeed that the CO displacement by the Cl atom is quite competitive with the direct hydrogen abstraction. Thus, when a methyl group is present in a substrate which undergoes a reaction with a radical, a substitution at the methyl carbon atom is in principle possible, irrespective of the multiplicity of the departing group.

The TS **Sub/4** involves the HCC terminal carbon, but again, it is not associated with a C_{3v} symmetry – while the C–C–C framework is bent by about 10°, both entering and departing groups are slightly deviated by 2° around the virtually planar methyl group. The ratio of both stretched distances C–H/C–C in **Sub/4** turns out to be in the same order of magnitude as that in typical C–H/C–C bond lengths (about 0.7). In contrast, the departing C–H distance in **Sub/5** is markedly longer than that in **Sub/4**. It is likely due to the difference in exothermicities of both reaction pathways. Again, because the acetylenic product $CH_3C{\equiv}CH + H$ **4** is more stable than its vinylidene isomer $CH_3CH{=}C + H$ **5, Sub/4** is expected to be energetically lower-lying than **Sub/5**. Note that in both TS's **Ab/3** and **Sub/5**, the HCC central carbon carries out an attack in a nearly perpendicular angle to the target.

Finally, we have also located the TS **Ins/6**, which characterizes an insertion of the HCC central carbon into a methane C–H bond. Attempts to locate a TS for insertion involving the HCC terminal carbon were not successful. The reason is probably the fact that this TS easily collapses into the TS for abstraction **Ab/2**, which is situated in the same region of the energy surface but which instead has a much lower energy. The product **6** is ethylcarbyne which normally exhibits a quartet ground state. The doublet excited state **6** is expected to be of high-energy and to readily rearrange into more stable isomers such as the methylvinyl radical, by simple 1,2-H shifts. It is relevant to note that the insertion of HC into a C–H bond of ethene giving allyl radical is essentially a barrier-free process [37].

With regard to energetic aspects, a rapid comparison of the results recorded in Fig. 5 clearly points out that the abstraction of a methane hydrogen by HCC terminal carbon, $\mathbf{HCC + CH_4 \rightarrow TS\ Ab/2 \rightarrow HCCH + CH_3}$, is by far the most favoured process. On the other hand, the H-abstractions are inherently more favorable than the radical substitutions irrespective of the attacking site. The insertion via **Ins/6** is an energy-demanding but reachable route. As stated above, the pathway leading to a vinylidene isomer is consistently more difficult to achieve than that to its acetylene counterpart.

Overall, it can be confirmed that the gas-phase reaction of the ethynyl radical with methane is a classical direct H-abstraction reaction. Our best estimate predicts an energy barrier of 10 kJ mol^{-1} for this motion. Use of the estimate in conjunction with the geometrical and vibrational parameters, allows the rate coefficient to be evaluated within the framework of the conventional transition state theory (TST). For CH_4 and C_2H, experimental rotational constants and frequencies were used, whereas for the transition structure the computed UMP2/6-31G(d,p) geometry and frequencies (scaled by 0.95) were adopted. All internal modes of the TS were treated as harmonic vibrations. Rotational symmetry numbers were not included, but a reaction path degeneracy of four was taken into account. Tunneling was treated by the Eckart equation [38]; this correction is small, ranging from a factor of 1.35 at 200 K to 1.01 at 2000 K. For an energy barrier of 10 kJ mol^{-1}, the theo-

retical k(TST) values for the 200–2000 K range can be represented by a modified Arrhenius expression $k(\mathrm{TST}) = 1.66 \times 10^{-17} T^{2.30\pm0.04} \exp[-(760 \pm 20)\ \mathrm{K}/T]$ cm^3 molecule^{-1} s^{-1}. The k (TST) is too small at the lower temperatures, by a factor of $\approx$4 at 300 K, and too large at higher temperatures, by a factor of $\approx$2 at 800 K. Clearly, the theoretical pre-exponential factor is overestimated by an order of magnitude. There are different reasons for such a variation: (i) some of the computed TS frequencies at the UMP2/6-31G(d,p) level are markedly too low; (ii) the problem of the linearity of TS **Ab/2** might be important; (iii) at the same time, the ab initio barrier height appears to be too high by about 3 or 4 kJ mol^{-1}; and (iv) due to the flatness of the potential energy surface in the saddle region, the classical TST treatment might be not appropriate; a variational TST treatment is likely to be needed. It is clear therefore that higher levels of theory in conjunction with larger basis sets are required for the characterization of the TS, together with the use of finer kinetic treatments, in order to derive quantitatively correct theoretical predictions of the kinetics of this reaction.

4. Concluding remarks

In the present study, the absolute rate coefficients of the gas-phase reaction of the ethynyl radical with methane ($HC{\equiv}C + CH_4$) were measured for the first time at higher temperatures. The result in the 295–800 K range can be expressed by: $k(T) = 1.39 \times 10^{-18} T^{2.34\pm0.40} \exp[(380 \pm 180)\,\mathrm{K}/T]$ cm^3 molecule^{-1} s^{-1}. Ab initio MO calculations up to the CCSD(T)/aug-cc-pVTZ//CCSD(T)/6-31G(d,p) level revealed that among the possible mechanisms of hydrogen abstraction, insertion and substitution reactions, the direct H-abstraction yielding $CH_3 + HC{\equiv}CH$ is associated with the lowest barrier height of $\leqslant 10$ kJ mol^{-1}.

Acknowledgements

The authors are indebted to the Fund for Scientific Research (FWO-Vlaanderen) and K.U. Leuven Research Council for continuing support.

References

[1] K.D. Tucker, M.L. Kutner, P. Thaddeus, Astrophys. J. 193 (1974) L115.
[2] W.M. Jackson, Y. Bao, R.S. Urdahl, J. Geophys. Res. 96 (1991) 1756.
[3] D. Toublanc, J.P. Parisot, J. Brillet, D. Gautier, F. Raulin, C.P. McKay, Icarus 2 (1995) 113.
[4] G.R. Gladstone, M. Allen, Y.L. Yung, Icarus 119 (1996) 1.
[5] B.J. Opansky, S.R. Leone, J. Phys. Chem. 100 (1996) 4888, 19904.
[6] R.J. Hoobler, B.J. Opansky, S.R. Leone, J. Phys. Chem. A 101 (1997) 1338.
[7] U. Bonne, K.H. Homann, H.Gg. Wagner, Symp. (Int.) Combust. [Proc.] 10 (1965) 503.
[8] J.D. Bittner, J.B. Howard, Symp. (Int.) Combust. [Proc.] 19 (1982) 211.
[9] J. Warnatz, Combust. Sci. Technol. 34 (1983) 177.
[10] J. Warnatz, Ber. Bunsenges. Phys. Chem. 87 (1983) 1008.
[11] H. Bockhorn, F. Fetting, H.W. Wenz, Ber. Bunsenges. Phys. Chem. 87 (1983) 1067.
[12] J.A. Kiefer, W.A. Von Drasek, Int. J. Chem. Kinet. 22 (1990) 747.
[13] R.P. Lindstedt, G. Skevis, Combust. Sci. Technol. 125 (1997) 73.
[14] C. Douté, J.-L. Delfau, C. Vovelle, Combust. Sci. Technol. 103 (1994) 153.
[15] M. Frenklach, H. Wang, Symp. (Int.) Combust. [Proc.] 23 (1990) 1559.
[16] D.R. Lander, K.G. Unfried, G.P. Glass, R.F. Curl, J. Phys. Chem. 94 (1990) 7759, and references therein.
[17] J. Peeters, H. Van Look, B. Ceursters, J. Phys. Chem. 100 (1996) 15124.
[18] D. Sengupta, J. Peeters, M.T. Nguyen, Chem. Phys. Lett. 91 (1998) 283.
[19] J.A. Miller, C.T. Bowman, Prog. Energy Combust. Sci. 15 (1989) 287.
[20] A.M. Tarr, O.P. Strausz, H.E. Gunning, Trans. Faraday Soc. 61 (1965) 1946.
[21] C.F. Cullis, D.J. Hucknall, J.V. Shepherd, Proc. Roy. Soc. A 335 (1973) 525.
[22] A.H. Laufer, J. Phys. Chem. 85 (1981) 3828.
[23] H. Okabe, J. Chem. Phys. 75 (1981) 2772.
[24] H. Okabe, J. Chem. Phys. 78 (1983) 1312.
[25] H. Okabe, Can. J. Chem. 61 (1983) 850.
[26] K. Devriendt, H. Van Look, B. Ceursters, J. Peeters, Chem. Phys. Lett. 261 (1996) 450.
[27] H. Van Look, J. Peeters, J. Phys. Chem. 99 (1995) 16284.
[28] J. Peeters, S. Vanhaelemeersch, J. Van Hoeymissen, R. Borms, D. Vermeylen, J. Phys. Chem. 93 (1989) 3892.
[29] J. Peeters, J. Van Hoeymissen, S. Vanhaelemeersch, D. Vermeylen, J. Phys. Chem. 96 (1992) 1257.
[30] K. Devriendt, J. Peeters, J. Phys. Chem. A 101 (1997) 2546.
[31] B. Ceursters, Ph.D. Thesis, K.U. Leuven, 2000.
[32] B. Ceursters, H.M.T. Nguyen, J. Peeters, M.T. Nguyen, Chem. Phys. 2000, submitted.

[33] M.J. Frisch et al., GAUSSIAN94, Revision E.2: Gaussian Inc., Pittsburgh PA, 1995.
[34] H. Kanamori, E. Hirota, J. Chem. Phys. 89 (1988) 3962.
[35] J.A. Litwinowicz, D.W. Ewing, S. Jurisevic, M.J. Manka, J. Phys. Chem. 99 (1995) 9709.
[36] R. Sumathi, M.T. Nguyen, J. Phys. Chem. 102 (1998) 8150.
[37] Z.X. Wang, M.B. Huang, Chem. Phys. Lett. 291 (1998) 381.
[38] J.I. Steinfeld, J.S. Francisco, W.L. Hase, Chemical Kinetics and Dynamics, second ed., Prentice-Hall, New York, 1999.